Channel Estimators for LTE-A Downlink Fast Fading Channels

Michael Meidlinger, Michal Šimko, Qi Wang and Markus Rupp
Institute of Telecommunications, Vienna University of Technology
Gusshausstrasse 25/389, A-1040 Vienna, Austria
Email: {mmeidlin, msimko, qwang, mrupp}@nt.tuwien.ac.at
Web: http://www.nt.tuwien.ac.at/research/mobile-communications

***Abstract*—In this paper, we present channel estimators for Long Term Evolution Advanced (LTE-A) fast fading channels. We show that the LTE-A Reference Signals (RS) structure—despite being designed for rather static scenarios—allows for accurate estimation performance even for higher speeds. We derive a Linear Minimum Mean Square Error (LMMSE) estimator and outline the restrictions that the LTE-A standard places on this estimator. Moreover, we present a novel Least Squares (LS) estimator based on a smoothness constraint, attempting to approach the performance of the LMMSE estimator, as our simulations reveal the rather limited capabilities of conventional interpolation techniques.**

I. Introduction

In Multi User (MU) Multiple-Input Multiple-Output (MIMO) transmissions, an evolved base station (eNodeB) transmits to different User Equipments (UEs) at the same time on the same frequency, multiplexing the individual streams purely in the spatial domain. In order to benefit from this additional degree of freedom, LTE-A base stations support transmit modes that allow to dynamically schedule users according to their time variant channels. Therefore, they are capable of changing the number of downlink transmission layers at certain frequencies and/or use non codebook based precoders to optimize throughput for any given channel realization [1]. While this approach strives to increases the overall system performance, it also leads to a granularization of the time frequency resource grid which needs to be taken into account by an appropriate RS structure and corresponding estimators.

In [2], we showed how UE-specific RS or Demodulation-RS (DM-RS) can be used to obtain estimates for LTE-A block fading channels. These estimators perform well up to a speed of around 50 km/h but become infeasible for UEs moving at a higher pace. Up to the authors' knowledge, there has been no work investigating the effects of high Doppler speed on LTE-A channel estimation. We therefore build on the results of [2] to derive estimators for fast fading scenarios. We introduce an LMMSE estimator which relies on perfect knowledge of the precoder and second order channel statistics. Even though such an estimator is impractical in real world scenarios, it is the optimum linear estimator minimizing the channel estimation Mean Square Error (MSE). Thus, we rather use it as a reference to be compared against more realistic Least Squares (LS) estimators. The underlying procedure is the same for all of these LS estimators: Given a limited number of channel estimates on pilot positions, more or less sophisticated interpolation techniques are employed to obtain an estimate of the full time and frequency selective channel. Investigating different interpolation techniques, we found that plain linear interpolation outperformed higher order interpolation techniques such as cubic spline interpolation. Consequently, we derive a novel LS interpolator based on a smoothness constraint in order to overcome the limited performance of linear interpolation.

The rest of this work is structured as follows: Section II gives an overview of the system model and explains how we can use the RS structure defined by the LTE-A standard [3]. Subsequently, Section III contains the analytical development of the LMMSE and LS estimators with respect to the LTE-A pilot structure. Eventually, Section IV will evaluate the performance and compare the different estimators by means of numeric simulations employing a standard compliant LTE-A Link-Level simulator [4]. All data is available online for reproducibility.

II. System Model

In fast fading scenarios, the MIMO channel is time as well as frequency dependent. Thus we define

$$\mathbf{H}^{(i,j)} := \begin{bmatrix} H_{1,1}^{(i,j)} & \dots & H_{1,N_{\text{time}}}^{(i,j)} \\ \vdots & \ddots & \vdots \\ H_{N_{\text{freq}},1}^{(i,j)} & \dots & H_{N_{\text{freq}},N_{\text{time}}}^{(i,j)} \end{bmatrix} \tag{1}$$

as the time and frequency dependent channel from transmit antenna j to receive antenna i, with N_{freq} and N_{time} being the total number of Orthogonal Frequency Division Multiplexing (OFDM) symbols in time and the number of subcarriers per Resource Block (RB), respectively. Similarly, we define $\mathbf{P}^{(k,l)}$ to be the (in general) time and frequency dependent precoder from transmit layer l to transmit antenna k. Please note that we do not make any assumptions about the precoder at all: In fact, one of the main reasons for using DM-RS is to overcome limitations of codebook based precoding.

ISBN 978-3-8007-3466-5

If we now set

$$\mathbf{H}_{i,j} := \operatorname{diag}\Big(\underbrace{\operatorname{vec}(\mathbf{H}^{(i,j)})}_{=:\mathbf{h}_{i,j}}\Big), \quad \mathbf{P}_{k,l} := \operatorname{diag}\Big(\underbrace{\operatorname{vec}(\mathbf{P}^{(k,l)})}_{=:\mathbf{p}_{k,l}}\Big), \tag{2}$$

and assemble all symbols to be transmitted in two consecutive RBs on all layers in the $N_{\text{freq}}N_{\text{time}}N_{\text{L}}$-dimensional vector $\mathbf{x}$, we can write the receive vector $\mathbf{y}$ as

$$\mathbf{y} = \mathbf{HPx} + \mathbf{n}, \tag{3}$$

where

$$\mathbf{H} = \begin{bmatrix} \mathbf{H}_{1,1} & \dots & \mathbf{H}_{1,N_{\text{TX}}} \\ \vdots & \ddots & \vdots \\ \mathbf{H}_{N_{\text{RX}},1} & \dots & \mathbf{H}_{N_{\text{RX}},N_{\text{TX}}} \end{bmatrix} \in \mathbb{C}^{N_{\text{freq}}N_{\text{time}}N_{\text{RX}} \times N_{\text{freq}}N_{\text{time}}N_{\text{TX}}},$$
$$\mathbf{P} = \begin{bmatrix} \mathbf{P}_{1,1} & \dots & \mathbf{P}_{1,N_{\text{L}}} \\ \vdots & \ddots & \vdots \\ \mathbf{P}_{N_{\text{TX}},1} & \dots & \mathbf{P}_{N_{\text{TX}},N_{\text{L}}} \end{bmatrix} \in \mathbb{C}^{N_{\text{freq}}N_{\text{time}}N_{\text{TX}} \times N_{\text{freq}}N_{\text{time}}N_{\text{L}}}, \tag{4}$$

$\mathbf{n}$ denotes i.i.d. Gaussian noise with covariance matrix $\sigma_n^2\mathbf{I}$ and $N_{\text{L}}, N_{\text{TX}}$ and N_{RX} are the number of transmit layers, transmit antennas and receive antennas, respectively. Since the DM-RS are inserted before the precoding, we actually attempt to estimate the product of precoder and channel matrix, $\mathbf{A} = \mathbf{HP}$. We call $\mathbf{A}$ the effective channel that—according to Equation (4)—also assumes block diagonal structure with the blocks $\mathbf{A}_{m,n} = \operatorname{diag}(\mathbf{a}_{m,n})$. Consequently, the composites $\mathbf{A}_{m,n}$ of channel and precoder linearly map transmit layer n to receive antenna m. Assuming a spatially uncorrelated channel, the estimation can be performed individually for each channel vector $\mathbf{a}_{m,n}$.

Figure 1 shows a pair of RBs in the time-frequency domain. Depending on the overall system bandwidth, the Physical Downlink Control Channel (PDCCH) can make up to the first four symbols in each subframe, thus limiting the Physical Downlink Shared Channel (PDSCH) to the region that is covered by DM-RS.

In [2], we showed that for the number of transmit layers $N_L \leq 4$, we can obtain the LS estimates at the pilot positions simply by taking the inner product between the received symbols and the corresponding orthonormal vector. In case of fast fading, $N_L \leq 4$ is necessary to preserve the orthogonality between the RS . The vector $\hat{\mathbf{a}}_{\text{p}}$ comprising the LS estimates on the pilot positions will be the starting point for the estimators presented in the subsequent sections. In the following, we will drop the indices m, n whenever there is no risk for confusion.

III. Channel Estimatiors

A. LS Estimators based on conventional 2D interpolation

1) Linear Interpolation: The simplest way to extend the estimates at the pilot positions $\hat{\mathbf{a}}^{\text{p}}$ to a full estimate $\hat{\mathbf{A}}$ is to use linear interpolation. The interpolated values lie on planes spanned through the three closest pilot symbols.

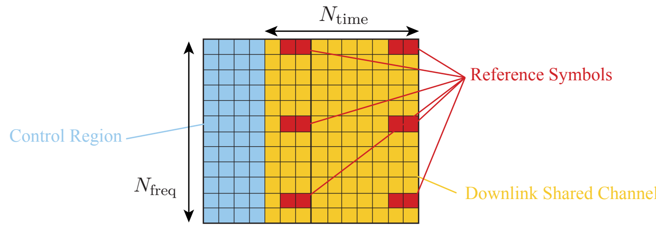

Fig. 1. RB pair in the time-frequency plane.

2) Cubic Spline Interpolation: Cubic spline interpolation attempts to improve the quality of linear interpolation by interconnecting the data points with polynomials of third order instead of straight planes. The additional unknowns (polynomial coefficients) can be obtained by claiming the interpolant to be two times continuously differentiable. Intuitively, we expected this approach to outperform linear interpolation, but a closer look at Figure 1 reveals why we were wrong: There is just too few pilots per RB pair. In fact, there is just two pilots in time and three pilots in frequency, all of them lying at the edge of the interpolation region, which leads to boundary effects distorting the result. This can be explained as follows: At the boundary of the interpolation interval one cannot calculate the derivatives of the interpolant. However, the algorithm calculating the interpolant needs this values so that the underlying linear equation system is not under determined. Usually the second derivatives at the interval borders are set to zero ("Natural Splines").

B. LMMSE Estimator

Now we intend to estimate the random vector $\mathbf{a}$, disturbed by the additive noise vector $\mathbf{v}$ given the LS estimate $\hat{\mathbf{a}}^{\text{p}}$ at the pilot positions. The well known linear estimator minimizing the MSE is then given as

$$\hat{\mathbf{a}}_{\text{LMMSE}} = \mathbf{R}_{\mathbf{a},\mathbf{a}^{\text{p}}}\big(\mathbf{R}_{\mathbf{a}^{\text{p}}} + \mathbf{R}_{\mathbf{v}}\big)^{-1}\hat{\mathbf{a}}^{\text{p}}, \tag{5}$$

with the respective cross- and autocorrelation matrices $\mathbf{R}_{\mathbf{a},\mathbf{a}^{\text{p}}}$, $\mathbf{R}_{\mathbf{a}^{\text{p}}}$ and $\mathbf{R}_{\mathbf{v}}$. Given the autocorrelation matrix of the channel vector $\mathbf{h}_{j,k}$, we can obtain the autocorrelation matrix of the effective channel vector $\mathbf{a}_{m,n}$ as

$$\begin{aligned} \mathbf{R}_{\mathbf{a}_{m,n},\mathbf{a}_{m,n}} &= \mathrm{E}\{\mathbf{a}_{m,n}\mathbf{a}_{m,n}^H\} \\ &= \mathrm{E}\left\{\sum_{j=1}^{N_{\text{TX}}}\mathbf{P}_{j,n}\mathbf{h}_{m,j}\left(\sum_{k=1}^{N_{\text{TX}}}\mathbf{P}_{k,n}\mathbf{h}_{m,k}\right)^H\right\} \\ &= \sum_{j=1}^{N_{\text{TX}}}\mathbf{P}_{j,n}\mathbf{R}_{\mathbf{h}}\mathbf{P}_{j,n}^H. \end{aligned} \tag{6}$$

In this derivation, we assumed that all channel vectors $\mathbf{h}_{i,j}$ have the same auto correlation matrix $\mathbf{R}_{\mathbf{h}}$ and are not correlated with each other. From [5] we know that

$$\mathbf{R}_{\mathbf{v}} = \mathbf{I}(\sigma_n^2 + \sigma_{\text{ICI}}^2). \tag{7}$$

ISBN 978-3-8007-3466-5

The inter carrier interference noise power for the case of Jake's spectrum is derived in [6] as

$$\sigma_{\mathrm{ICI}}^2 = 1 - \int_{-1}^{1} (1-|x|) J_0(\omega_{\mathrm{D}} T_{\mathrm{s}} x)\,\mathrm{d}x\ , \tag{8}$$

where $J_0(\cdot)$ denotes the zeroth-order Bessel function, ω_{D} is the radian Doppler frequency and T_{s} is the duration of an OFDM symbol.

As stated before, one of the reasons why DM-RS were introduced was to allow for non codebook based precoding without additional signalling. As a result, the use of the LMMSE estimator is restricted to the following scenarios:

1) The estimator of Equation (5) together with the results of Equations (6)–(8) yield the optimum linear estimator in the MSE sense. Even though the precoders will not be known in practical systems, we can use it in our simulations to obtain a lower bound on the MSE of the LS estimators.
2) In practical systems correlation values need to be estimated when using an LMMSE estimator. This is usually done by time averaging, exploiting the ergodicity of the channel. Therefore, an estimate

$$\hat{\mathbf{R}}_{\mathbf{a}} = \frac{1}{N_{\mathrm{real}}} \sum_{r=1}^{N_{\mathrm{real}}} \hat{\mathbf{a}}\hat{\mathbf{a}}^H \tag{9}$$

of $\mathbf{R}_{\mathbf{a}}$ could be used in Equation (5), thus eliminating the dependence on precoder knowledge. However, as we can see from Equation (6), the correlation of the effective channel is significantly impacted by the precoder. Without further provisions (e.g., limiting the precoder's temporal rate of change and scheduling arrangments that are constant over several subsequent subframes) ergodicity and a sufficient number of realizations N_{real} is not guaranteed.

C. Smoothness Estimator

The fact that the LS estimators in Section III-A work best with linear interpolation but are still far from the performance of the LMMSE estimator in Section III-B gave rose to the question whether it is possible to find a more suitable interpolation technique for the given pilot pattern. Since the desired channel smoothness could not be achieved with spline interpolation, we formulated the following optimization problem:

$$\begin{aligned}
&\text{Minimize}\\
&\quad \lambda_F \sum_{f,t} |U_{f+1,t} - U_{f,t}|^2 + \lambda_T \sum_{f,t} |U_{f,t+1} - U_{f,t}|^2\\
&\text{Subject to}\\
&\quad U_{f,t} = \hat{A}^{\mathrm{p}}_{f,t} \quad \text{for } (f,t) \in \mathcal{P}\\
&\quad \lambda_T > 0\\
&\quad \lambda_F > 0
\end{aligned} \tag{10}$$

Here the matrix $\mathbf{U}$ comprising the elements $U_{t,f}$ is a matrix over time and frequency, just like $\mathbf{H}^{(i,j)}$ in Equation (1) and $\mathcal{P}$ denotes the set of pilot indices. The objective function in Equation (10) is essentially the discrete version of the norm of the weighted gradient

$$\int_{f,t} \left\| \boldsymbol{\lambda} \cdot \boldsymbol{\nabla} u(f,t) \right\|^2 \mathrm{d}(f,t)\,. \tag{11}$$

Hence, the optimum $\mathbf{U}_{\mathrm{opt}} = \hat{\mathbf{A}}_{\mathrm{SM}}$ will have the smallest possible variations over the RB pair while still matching the LS estimate at the pilot positions. Equation (10) is a convex optimization problem in $\mathbf{U}$ and $\boldsymbol{\lambda} = \begin{bmatrix}\lambda_F & \lambda_T\end{bmatrix}^T$ which can be solved efficiently using `cvx` [7].

As our simulations have shown (cf. Section IV), the solution of Equation (10) for any SNR and UE speed is (up to numerical inaccuracies) identical to that of the slightly different convex optimization problem

$$\begin{aligned}
&\text{Minimize}\\
&\quad \sum_{(f,t)\in\mathcal{P}} |\hat{A}^{\mathrm{p}}_{f,t} - U_{f,t}|^2 + \lambda_F \sum_{f,t} |U_{f+1,t} - U_{f,t}|^2\\
&\qquad\qquad + \lambda_T \sum_{f,t} |U_{f,t+1} - U_{f,t}|^2\\
&\text{Subject to}\\
&\quad \lambda_T > 0\\
&\quad \lambda_F > 0
\end{aligned} \tag{12}$$

which allows for a deviation of the interpolant at the pilot positions but penalizes them in the objective function. However, if we assume $\boldsymbol{\lambda}$ to be constant in Equation (12), this convex optimization problem boils down to an LS problem whose closed form solution we calculated to be

$$\hat{\mathbf{a}}_{\mathrm{SM}} = \mathrm{vec}\big(\hat{\mathbf{A}}_{\mathrm{SM}}\big) = \Big(\big(\lambda_F \mathbf{F} \oplus \lambda_T \mathbf{T} + \mathbf{D}\big)^{-1}\Big)_{\mathrm{p}} \hat{\mathbf{a}}^{\mathrm{p}} = \mathbf{S}\hat{\mathbf{a}}^{\mathrm{p}} \tag{13}$$

with

$$\begin{aligned}
\mathbf{F} &= \underbrace{\begin{bmatrix} 1 & -1 & & & \\ -1 & 2 & -1 & & \\ & \ddots & \ddots & \ddots & \\ & & -1 & 2 & -1 \\ & & & -1 & 1 \end{bmatrix}}_{N_{\mathrm{freq}} \times N_{\mathrm{freq}}},\\
\mathbf{T} &= \underbrace{\begin{bmatrix} 1 & -1 & & & \\ -1 & 2 & -1 & & \\ & \ddots & \ddots & \ddots & \\ & & -1 & 2 & -1 \\ & & & -1 & 1 \end{bmatrix}}_{N_{\mathrm{time}} \times N_{\mathrm{time}}},\\
\mathbf{D} &= \mathrm{diag}\big(\boldsymbol{\Pi}\big), \qquad \Pi_k := \begin{cases} 1 & k \text{ is a pilot position} \\ 0 & \text{otherwise} \end{cases},
\end{aligned} \tag{14}$$

where $\oplus$ denotes the Kronecker sum $\lambda_F \mathbf{F} \oplus \lambda_T \mathbf{T} = \mathbf{I}_{N_{\mathrm{time}}} \otimes \lambda_F \mathbf{F} + \lambda_T \mathbf{T} \otimes \mathbf{I}_{N_{\mathrm{freq}}}$ and the notation $(\mathbf{M})_{\mathrm{p}}$ indicates that the matrix $\mathbf{M}$ is reduced to those columns where pilot symbols are present.

The closed form expression Equation (13) can be used to reduce computational complexity inherent to numerical

ISBN 978-3-8007-3466-5

convex optimization. First of all, the matrix to be inverted has band structure with five nonzero diagonals spanning a total bandwidth of $B_W = 2N_{\text{freq}} + 1$. Moreover, the matrix is independent of the channel estimates and solely a function of $\boldsymbol{\lambda}$. As we will see from simulations in Section IV, $\boldsymbol{\lambda}$ is approximately constant for given UE speeds, SNR and channel model. As a result, we can reuse the filtering matrix $\mathbf{S}$ without recalculating it for any pair of RBs.

IV. Simulation Results

In this section, we present numerical results from a standard compliant LTE-A Link-Level Simulator [4]. We carried out Monte Carlo simulations, using a 4×4 single user transmission setup with non identity precoding and the ITU VehA frequency selective channel model with Jake's spectrum. Respective parameters can be found in Table I.

TABLE I
Simulation Parameters

Parameter	Figure 2	Figures 3 and 4
SNR	15dB	—
UE speed	—	100km/h
CQI	—	9
HARQ retransmissions	—	3
Bandwidth	1.4 MHz	1.4 MHz
Carrier frequency	2.1 GHz	2.1 GHz

Figure 2 shows the MSE as a function of UE speed. As stated above, RB based spline interpolations performs worse than linear interpolation. As we can see from this figure, the proposed smoothness interpolation technique outperforms the linear one.

Figure 3 depicts the SNR dependency of the MSE. The results look similar to Figure 2 with respect to estimator performance, the difference being that the smoothness interpolator saturates for high SNR and becomes worse than the estimators based on conventional interpolation techniques.

Please note that the curve for the smoothness interpolator in Figures 2 and 3 is actually three curves plotted on top of each other, each of which represents a different implementation of the estimator:

1) Interpolation based on Equation (10)
2) Interpolation based on Equation (12)
3) Interpolation based on Equation (13), where the filter matrix $\mathbf{S}$ has been calculated just once for each SNR and UE speed and has then been reused for interpolation of all RBs on all layers.

This results indicate that the proposed smoothness interpolator can be implemented efficiently without significant loss of performance.

Looking at Figure 4, we can see how the MSE error performance translates into coded throughput. The proposed smoothness estimator achieves a SNR gain of roughly 0.5 dB in the range of practical relevant SNR.

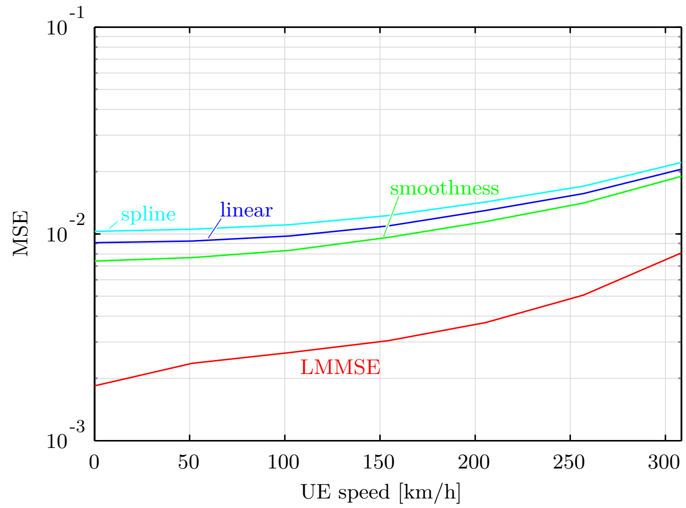

Fig. 2. Channel estimation MSE as a function of UE speed with SNR = 15 dB.

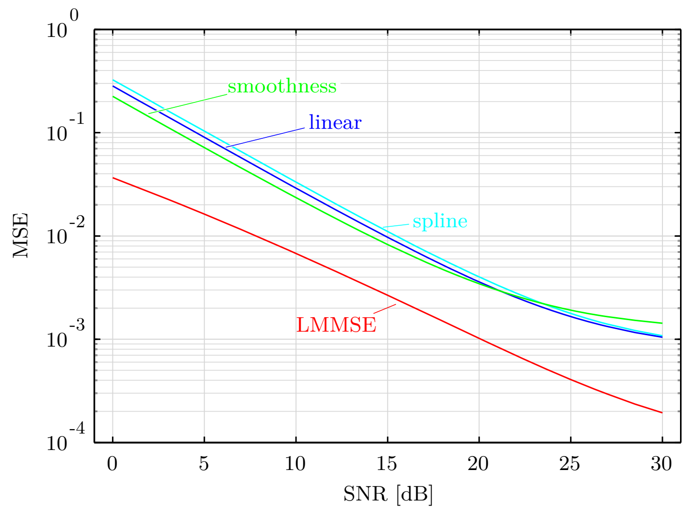

Fig. 3. Channel estimation MSE as a function of SNR at an UE speed of 100 km/h.

V. Conclusion and Outlook

In this work, we derived channel estimators for LTE-A fast fading channels. We demonstrated that for this case, the well known estimation strategies for LTE are either hard to implement (LMMSE estimator) or provide limited performance (LS estimators based on linear interpolation). To overcome these drawbacks, we proposed a novel LS estimator based on a smoothness constraint, providing a SNR gain of 0.5 dB. Since the filtering matrix that we employ for this estimator is approximately constant for given SNR and UE speeds, the complexity of the estimator is comparable to simple linear interpolation.

We also want to stress that the proposed interpolation technique can be generalized to arbitrary 2D interpolation problems where the underlying function is known to have a smooth shape.

ISBN 978-3-8007-3466-5

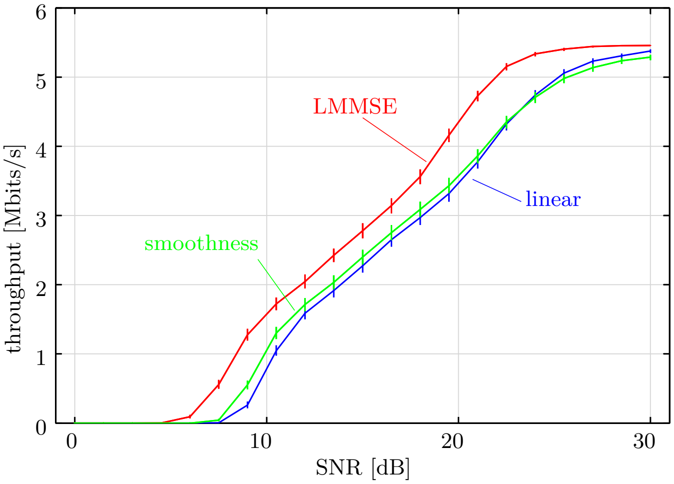

Fig. 4. Coded throughput. We transmitted 1500 subframes and calculated the 95% confidence intervals as shown above.

VI. Acknowledgement

The authors would like to thank the LTE research group for continuous support and lively discussions. Furthermore, the authors want to thank Prof. C. Mecklenbräuker for his suggestions and advice. This work has been funded by the Christian Doppler Laboratory for Wireless Technologies for Sustainable Mobility and A1 Telekom Austria AG. The financial support by the Federal Ministry of Economy, Family and Youth and the National Foundation for Research, Technology and Development is gratefully acknowledged.

References

[1] J. Duplicy, B. Badic, R. Balray, R. Ghaffar, P. Horáth, F. Kaltenberger, R. Knopp, I. Z. Kovács, H. T. Nguyen, D. Tandur, and G. Vivier, "MU-MIMO in LTE Systems," *EURASIP Journal on Wireless Communications and Networking*, vol. 2011.

[2] M. Meidlinger and Q. Wang, "Performance Evaluation of LTE Advanced Downlink Channel Estimators," in *19th International Conference on Systems, Signals and Image Processing (IWSSIP)*, April 2012, pp. 252 –255.

[3] 3GPP, "Technical Specification Group Radio Access Network; Physical Channels and Modulation; (Release 10)," Tech. Rep., Dec. 2010. [Online]. Available: http://www.3gpp.org/ftp/Specs/html-info/36211.htm

[4] C. Mehlführer, J. C. Ikuno, M. Šimko, S. Schwarz, M. Wrulich, and M. Rupp, "The Vienna LTE Simulators - Enabling Reproducibility in Wireless Communications Research," *EURASIP Journal on Advances in Signal Processing*, vol. 2011.

[5] M. Simko, Q. Wang, and M. Rupp, "Optimal pilot symbol power allocation under time-variant channels," *EURASIP Journal on Wireless Communications and Networking*, vol. 225, 2012.

[6] Y. Li and J. Cimini, L.J., "Bounds on the interchannel interference of OFDM in time-varying impairments," *IEEE Transactions on Communications*, vol. 49, no. 3, pp. 401 –404, March 2001.

[7] I. CVX Research, "CVX: Matlab software for disciplined convex programming, version 2.0 beta," http://cvxr.com/cvx, Sep. 2012.

ISBN 978-3-8007-3466-5